

# Delving deeper into CAR T cell evaluation

## A 3D imaging workflow to study the infiltration potential of CAR T cells into solid tumors

### Introduction

Profound analysis of tumor physiology and distribution of anti-tumor CAR T cells in the tumor microenvironment (TME) requires comprehensive 3D imaging data. Common 2D histological and IHC microscopy techniques are not sufficient for this purpose as they are usually applied to a limited number of thin sections which leads to the potential risk of missing relevant information. Tissue clearing, combined with light sheet microscopy, has the potential to bridge this technological gap and enable single-cell resolution imaging of whole large samples, including solid tumors or even entire organisms. However, technically challenging instruments and the use of homemade, difficult-to-reproduce immunostaining and clearing protocols currently pose significant obstacles to the establishment of this workflow in the context of pre-clinical studies. Here, we showcase the efficacy of 3D fluorescence microscopy using the UltraMicroscope Blaze™ for analyzing CAR T cells in solid tumors, employing pancreatic carcinoma xenografts as a model. By using automated light sheet microscopy along with validated antibodies, straightforward tissue clearing, and immunolabeling protocols, we can visualize<sup>1,2,3</sup> and quantify multiple tumor parameters and the infiltration of therapeutic CAR T cells at a cellular level. Hence, this workflow facilitates the unbiased evaluation of cellular therapies in large, heterogeneous samples like solid tumors and the TME.

### Background

In light sheet microscopy, the optical pathways for fluorescence excitation (horizontal) and detection (vertical) are decoupled (fig. 1). A laser light sheet is directed perpendicular to the observation axis, selectively exciting a single plane of the labeled sample. Illuminating only a thin layer along the z-axis produces high-resolution images with minimal and strictly localized photodamage and bleaching effects, unlike traditional epifluorescence microscopy techniques. By moving the sample along the z-axis through the light sheet, a series of images can be generated, forming a stack that enables the visualization of large biological samples in 3D with single-cell resolution. Imaged samples can range from small organoids and rodent organs to larger entities like whole mouse models or human kidneys.

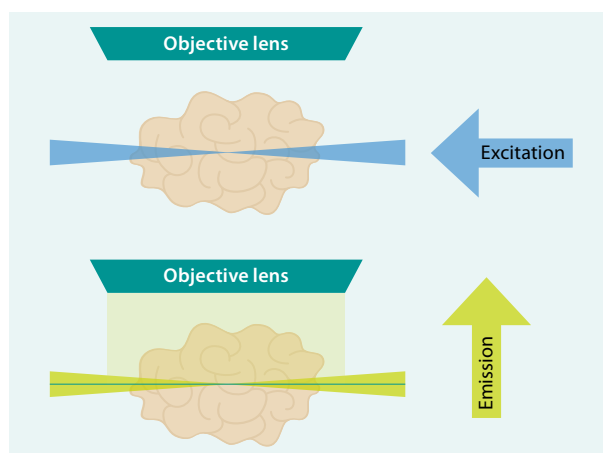


**Figure 1:** Samples are illuminated from the side by a focused light sheet while the fluorescence light is collected by an objective lens perpendicular to the illumination plane. 3D image stacks are generated by moving the sample through the light sheet.

## Materials and methods

### 1. Generation of pancreatic cancer xenografts

Human-derived xenograft models of pancreatic cancer were generated by subcutaneous injections of tumor cells (AsPC1, human pancreatic tumor cell line) into nonobese diabetic/severe combined immunodeficiency (NOD/SCID) mice (Jackson Laboratory, provided by Charles River). When tumors reached a size of  $>25 \text{ mm}^2$ , mice were randomized and treated intravenously with freshly prepared CAR T cells as follows: 1) therapeutic EGFR CAR T cells specifically targeting the pancreatic cancer xenografts, and 2) control BDCA-2 CAR T cells that do not specifically target the pancreatic tumor cells and, therefore, do not colocalize with the tumor ( $n = 7$  each).

### 2. 3D imaging workflow

The 3D imaging workflow is based on three main steps: 1) immunostaining, 2) tissue clearing, and 3) 3D light sheet imaging (fig. 2).

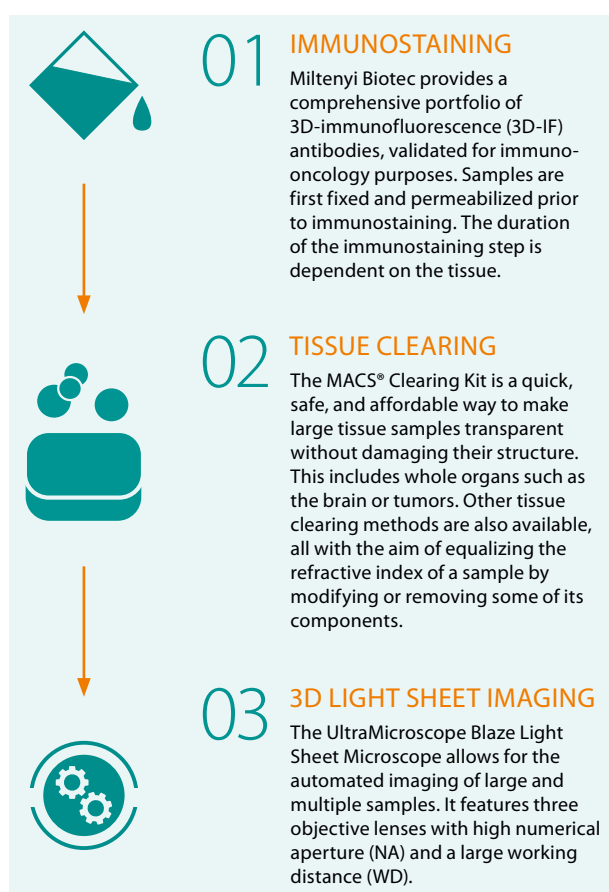


**Figure 2:** The 3D imaging workflow.

#### 2.1. Immunostaining

Vascular networks of tumors were stained *in vivo* using rhodamine lectin (Vector Laboratories). A 50  $\mu\text{L}$  injection of rhodamine lectin was administered intravenously, 5 minutes before euthanasia. The tumors were then excised and fixed by overnight incubation at  $2-8^\circ\text{C}$  in a 4% PFA buffer. To remove any remaining PFA, the tumors were washed three times in PBS. Subsequently, the tumors were permeabilized using 5 mL of Permeabilization Solution (MACS® Clearing Kit, Miltenyi Biotec) per sample, at room temperature, for 24 hours. The tumors were then stained with CD3 Antibody (anti-human, Vio® R667, REAfinity™,

REA613, Miltenyi Biotec) in Antibody Staining Buffer (MACS Clearing Kit, Miltenyi Biotec) for 7 days, with gentle shaking, at  $37^\circ\text{C}$ . To remove any unbound antibody, the stained tissues were washed three times in Antibody Staining Buffer for at least 4 hours each, at room temperature, using a rotating MACSmix™ Tube Rotator. Finally, the stained tissues were dehydrated by incubating them in increasing concentrations of ethanol (30% to 100%) for at least 4 hours at room temperature, with gentle and continuous rotation.

#### 2.2. Tissue clearing

Tissue clearing was performed by incubating the samples in 5 mL of MACS Clearing Solution (MACS Clearing Kit, Miltenyi Biotec) for a minimum of 6 hours at room temperature, with gentle and continuous rotation.

#### 2.3. 3D light sheet imaging

Cleared tumors were placed in the imaging chamber of the UltraMicroscope Blaze Light Sheet Microscope (Miltenyi Biotec) filled with MACS Imaging Solution (Miltenyi Biotec). Z-stacks were acquired depending on the sample size, at either  $1\times$  or  $4\times$  magnification with a step size of  $0.6 \mu\text{m}$ ,  $1.66 \mu\text{m}$ , or  $4 \mu\text{m}$ . The channels used were 488 nm for background signal (autofluorescence), 561 nm for rhodamine lectin staining, and 640 nm for staining with CD3 Antibody (anti-human, Vio R667, REAfinity, REA613). Analysis of the images was performed using Imaris 9.5.1v and ImageJ 1.49v software. This included 3D rendering, determination of tumor surface and volume, and identification of CD3-positive areas and vessels. CD3-positive areas were color-coded based on their location relative to the tumor surface or cell density. The proximity of vessels to each other and the size of the tumor determined the maximum distance for analysis. ImageJ 1.49v software was used to examine the gray values of CD3 and rhodamine lectin staining within the middle third of the tumors at maximum projection.

LEARN MORE



Check out our 3D-IF antibody portfolio.

► [miltenyibiotec.com/3D-IF-antibodies](https://miltenyibiotec.com/3D-IF-antibodies)

LEARN MORE



To access additional details on the sample preparation steps, please refer to our application protocol.

► [miltenyibiotec.com/clearing-tumors](https://miltenyibiotec.com/clearing-tumors)

LEARN MORE



Ready to dive into the 3rd dimension? Learn more about our easy-to-use light sheet microscope.

► [miltenyibiotec.com/ultramicroscope-blaze](https://miltenyibiotec.com/ultramicroscope-blaze)

## Results

By employing immunostaining, tissue clearing, and 3D light sheet imaging on pancreatic xenografts, a detailed and comprehensive 3D dataset was generated. These data helped evaluate the efficacy of potential cellular therapies by assessing parameters such as CAR T cell infiltration into solid tumors and their proximity to blood vessels.

### 3D imaging workflow allows for comprehensive analysis of large pancreatic carcinoma xenografts.

The 3D data obtained from rhodamine-lectin-labeled samples revealed the presence of chaotic, irregular, and highly branched vascular structures, which are characteristic of angiogenic vasculature within tumors exhibiting high heterogeneity (fig. 3, magenta). The UltraMicroscope Blaze's capability to image large volumes at single-cell resolution enabled the identification and analysis of individual T cells throughout the entire tumor tissue (fig. 3, cyan). Tumors treated with therapeutic EGFR CAR T cells displayed a higher presence of T cells compared to tumors treated with control BDCA-2 CAR T cells. In both groups, a large number of T cells were found near large blood vessels.

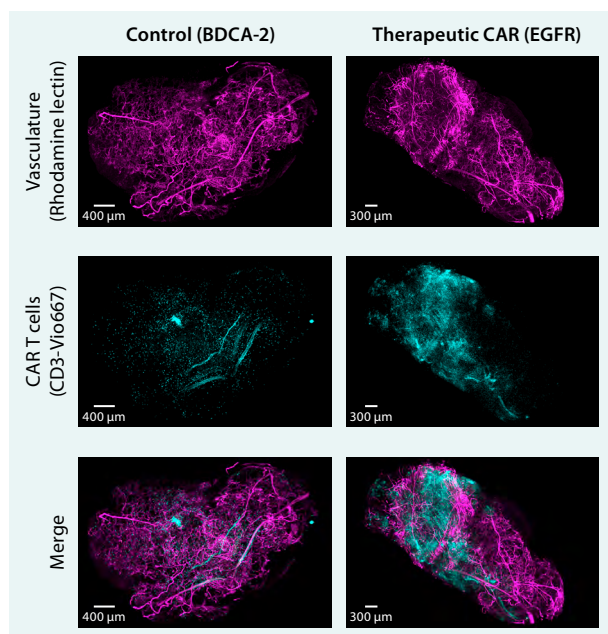


**Figure 3: CAR T cells infiltrating solid tumor tissues.** 3D images acquired with the UltraMicroscope Blaze showing pancreatic carcinoma xenografts treated with non-targeted BDCA-2 CAR T cells (left column), and therapeutic EGFR CAR T cells (right column). Rhodamine lectin staining was used to visualize the tumor vasculature (magenta), and CD3 Antibody (anti-human, Vio R667, REAfinity, REA613) was employed to label T cells (cyan).

### Light sheet profiling of tumor-infiltrating T cells reveals high frequency of T cells in the tumor periphery.

Tumor tissues and infiltrating CAR T cells were reconstructed and analyzed in 3D. The distribution of gray values throughout the tumor volume in the CD3 staining revealed that most of the T cells were located near the tumor surface. Notably, the therapeutic EGFR CAR T group demonstrated the highest tumor infiltration compared to the control BDCA-2 group (fig. 4A). Additional analysis utilizing spot detection function for CD3-positive cells confirmed higher infiltration in the EGFR group but revealed challenges in reaching the core of the solid tumor for both treatment groups.

Specifically, the EGFR-treated groups exhibited an increased number of CD3-positive cells starting from 100  $\mu\text{m}$  below the tumor surface (fig. 4B). However, beyond a distance of 400–500  $\mu\text{m}$  inward, both BDCA-2 and EGFR CAR T cells displayed comparable infiltration frequencies (fig. 4B). The relative frequency of CD3-positive cells in relation to the distance from the closest vessel was also assessed, indicating that while therapeutic EGFR CAR T cells managed to migrate from the blood vessels into the tumor, their progression within the tumor was still limited. Conversely, the control BDCA-2 group primarily accumulated near the blood vessels and failed to migrate further into the tissue.

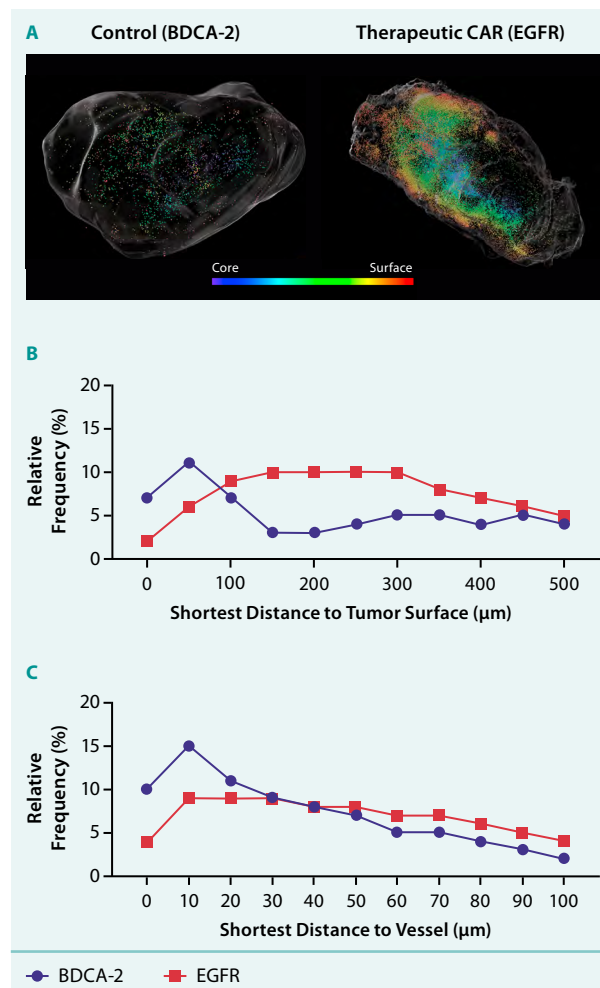


**Figure 4: Evaluation of the ability of CAR T cells to infiltrate solid tumors.** 3D reconstruction of solid tumor surface and infiltrating CAR T cells at day 6 after therapy start. T cell localization is color-coded, with red indicating a location closer to the tumor surface and blue at the core. CD3-positive T cells distribute in a spatially heterogeneous, island-like way within the tumor, with cells residing primarily in the outer tumor layers (A). Relative frequency of tumor-infiltrating spot-reconstructed CD3-positive cells in the tumor, with 0 representing the tumor surface (B). Distance of spot-reconstructed CD3-positive cells to the vasculature, with 0 representing a volume-reconstructed vessel surface ( $n = 1/\text{group/day}$ ) (C).

VIDEO



View the datasets presented in this study as a video:

► [miltenyibiotec.com/CAR-T-infiltrating-pancreatic-tumor](https://miltenyibiotec.com/CAR-T-infiltrating-pancreatic-tumor)

## Discussion

Image-based preclinical screenings traditionally rely on histology and 2D microscopy techniques, which utilize thin tissue sections from selected areas to evaluate complex and heterogeneous samples like solid tumors and their microenvironment. Unfortunately, this method doesn't allow for a complete and thorough grasp of the sample being studied. This could potentially harm the results of early trials and lead to a significant waste of time and resources. 3D imaging provides a solution to overcome this challenge.

The implementation of the 3D imaging workflow offers significant benefits to researchers involved in validating candidate cellular therapies. One major advantage is the early identification of the most promising CAR cell lines during preclinical studies. Making profound decisions at an early stage significantly reduces the risk of investing resources in less effective cell lines. By utilizing light sheet microscopy for validation purposes, researchers can select CAR T cell lines that exhibit enhanced infiltration capabilities into solid tumors, leading to cost and time savings, and more comprehensive results.

Researchers often hesitate to adopt 3D light sheet imaging due to concerns about laborious clearing protocols, validating antibodies for whole tissue labeling compatible with the clearing method, and handling a complex microscope. To address these challenges, we offer a simple and tested workflow consisting of an easy-to-use tissue clearing kit, our validated antibodies for whole organ labeling, a highly automated light sheet microscope, and step-by-step protocols for dedicated samples. The UltraMicroscope Blaze stands out as an ideal choice to image large samples up to whole organs or even an entire mouse. Researchers can efficiently operate the microscope without extensive training or expertise. Its automated functions ensure that even non-experts can use it effectively in a reproducible way, streamlining the imaging process and allowing researchers to focus on the analysis and interpretation of their results rather than the establishment of methods.

Finally, it is important to note that while the presented example focuses on CAR T cells, the application of light sheet microscopy extends to various cell types. The workflow's versatility enables its utilization in different contexts such as neuroscience, immuno-oncology, and drug biodistribution studies. We live in a 3D world, why not analyze it as such if you can?

## Conclusion

- 3D light sheet imaging offers a valuable alternative to traditional histology and microscopy techniques in preclinical screenings, addressing the challenges associated with evaluating complex 3D samples such as solid tumors and their microenvironment.
- Implementing the 3D imaging workflow in CAR T cell evaluation results in cost and time savings by providing researchers an unbiased, reliable tool to identify the best therapeutic CAR T cell candidates against solid tumors and discard less effective cell lines as early as possible.
- Light sheet microscopy is a versatile imaging technique applicable to various cell types and research areas, from CAR T cells to blood vessels, from immuno-oncology to neuroscience.
- Our user-friendly 3D imaging workflow and fully automated UltraMicroscope Blaze overcomes concerns about laborious protocols and complex instruments, making 3D light sheet imaging accessible and reproducible to everyone.

## References

1. Mohr, H. *et al.* (2021) *Cancers* 13: 126.
2. Taranda, J. and Turcan, S. (2021) *Cancers* 13: 1897.
3. Hahn, A. *et al.* (2021) *J. Theor. Biol.* 494: 110230.
4. Dobosz, M. *et al.* (2014) *Neoplasia* 16: 1–13.
5. Liu, Z. and Li, Z. (2014) *Theranostics* 4: 990–1001.
6. Pfeifer, R. *et al.* (2022) *Theranostics* 12(11) 4834–4850.



**Miltenyi Biotec B.V. & Co. KG** | Phone +49 2204 8306-0 | Fax +49 2204 85197 | [macsde@miltenyi.com](mailto:macsde@miltenyi.com) | [www.miltenyibiotec.com](http://www.miltenyibiotec.com)

Miltenyi Biotec provides products and services worldwide. Visit [www.miltenyibiotec.com/local](http://www.miltenyibiotec.com/local) to find your nearest Miltenyi Biotec contact.

Unless otherwise specifically indicated, Miltenyi Biotec products and services are for research use only and not for therapeutic or diagnostic use. Blaze, MACS, the Miltenyi Biotec logo, REAfinity, and Vio are registered trademarks or trademarks of Miltenyi Biotec B.V. & Co. KG and/or its affiliates in various countries worldwide. Copyright © 2023 Miltenyi Biotec and/or its affiliates. All rights reserved.